FINAL REPORT FOR NASA GRANT NAG1-1802

COMPUTATIONAL INVESTIGATIONS OF NOISE SUPRESSION IN SUBSONIC ROUND JETS

Principal-Investigator

Dr. C. David Pruett
Department of Mathematics
MSC 7803
James Madison University
Harrisonburg, VA 22807
(540) 568-6227 (WORK)
(540) 568-6857 (FAX)
dpruett@math.jmu.edu

NASA Technical Monitor

Dr. Kristine R. Meadows
Aeroacoustics Branch
MS 461 NASA
Langley Research Center
Hampton, VA 23681-0001
(757) 864-3624

Background

NASA Grant NAG1-1802, originally submitted in June 1996 as a two-year proposal, was awarded one-year's funding by NASA LaRC for the period 5 Oct., 1996, through 4 Oct., 1997. Because of the inavailability (from IT at NASA ARC) of sufficient supercomputer time in fiscal 1998 to complete the computational goals of the second year of the original proposal (estimated to be at least 400 Cray C-90 CPU hours), those goals have been appropriately amended, and a new proposal has been submitted to LaRC as a follow-on to NAG1-1802. The current report documents the activities and accomplishments on NAG1-1802 during the one-year period from 5 Oct., 1996, through 4 Oct., 1997.

NASA Grant NAG1-1802, and its predecessor, NAG1-1772, have been directed toward adapting the numerical tool of Large-Eddy Simulation (LES) to aeroacoustic applications, with particular focus on noise suppression in subsonic round jets. In LES, the filtered Navier-Stokes equations are solved numerically on a relatively coarse computational grid. Residual stresses, generated by scales of motion too small to be resolved on the coarse grid, are modeled. Although most LES incorporate spatial filtering, time-domain filtering affords certain conceptual and computational advantages, particularly for aeroacoustic applications. Consequently, this work has focused on the development of subgrid-scale (SGS) models that incorporate time-domain filters. The author is unaware of any previous attempt at purely time-filtered LES; however, Aldama [1] and Dakhoul and Bedford [3] have considered approaches that combine both spatial and temporal filtering. In our view, filtering in both space and time is redundant, because removal of high frequencies effects the removal of small spatial scales and vice versa.

1 Accomplishments

Most of the effort of NAG1-1772 was devoted to definition of a test case for axisymmetric-jet flow, to computation of the (laminar) base state for axisymmetric-jet flow (Pruett [19]), to adaptation of the direct numerical

simulation (DNS) algorithm of Pruett et al. [18] to the jet-flow problem of interest, and to installation of the subgrid-scale (SGS) model of Erlebacher et. al [4] (with a temporal filter) into the code to afford a baseline LES capability. These efforts were successful; however, as expected, the baseline model was overly dissipative, which suggested that dynamic modeling would be necessary as anticipated.

Most of the previous year's effort was devoted to an attempt to develop an efficient dynamic SGS model based on a temporal filter.

TIME-DOMAIN FILTER: An early priority of the previous effort was to development a candidate temporal filter. During this grant period, some effort was devoted to refinement of the filter. Time-domain filters fall into either of two broad categories: causal or acausal. For application to LES, only causal filtering is realizable. By definition, causal filters incorporate present and past information only, the future being inaccessible. Following Press et al. [17] and Strum and Kirk [24], we exploit the following linear acausal digital filter

$$\overline{s}_l = \sum_{j=0}^{m} p_j s_{l-j} + \sum_{k=1}^{n} q_k \overline{s}_{l-k} \tag{1}$$

where $s_l = s(t_l)$ is the raw discretized signal, $\overline{s}_l$ is the filtered signal, $t_l = l\Delta t$, Δt is the (constant) time interval between samples, and coefficients p_j and q_k are determined to give the filter certain desirable properties, which will be addressed subsequently. The filter of Eq. 1 is "nonrecursive" if $q_k = 0$ for all k and "recursive" if, for at least one k, $q_k \neq 0$, in which case the current value of the filtered quantity is a linear combination of past and present unfiltered values and past filtered values.

It is instructive to examine the frequency response of the filter associated with Eq. 1. From Press et al. [17], the transfer function, which quantifies the frequency response, is given by

$$H(\Omega) = \frac{\sum_{j=0}^{m} p_j e^{-ij\Omega}}{1 - \sum_{k=1}^{n} q_k e^{-ik\Omega}} \tag{2}$$

where $i = \sqrt{-1}$, $\Omega = \omega^* \Delta t^*$ is the dimensionless frequency, $\omega^* = 2\pi f^*$ is the dimensional circular frequency, and f^* is the dimensional physical frequency. (Throughout this work, we denote dimensional quantities by asterisk.) In

general, the frequency response of a recursive filter is related to a rational polynomial in the complex variable $1/\zeta$, where $\zeta = e^{i\Omega}$. The rational polynomial form of the transfer function allows considerable latitude in shaping the frequency response. Figure 1 below compares the modulus of the transfer function of prototypical low-pass digital recursive filters with that of an idealized "spectral cutoff" filter.

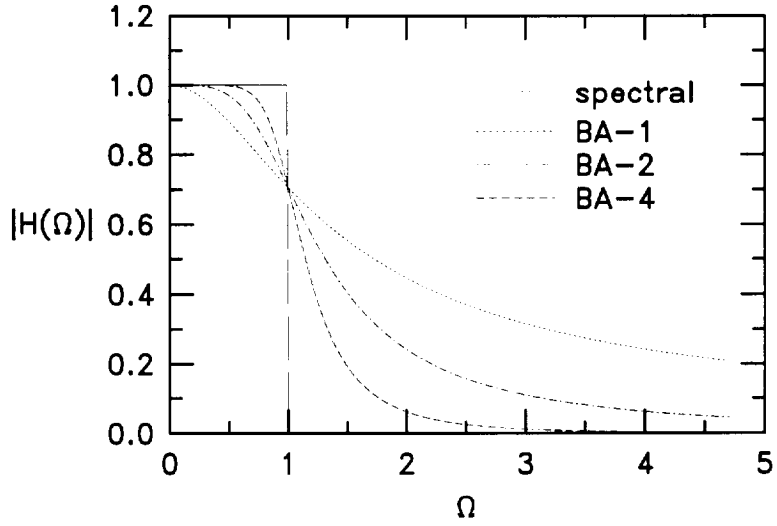

Transfer function of prototype first-, second-, and fourth-order causal digital filters compared with spectral-cutoff transfer function.

Note that, for the spectral cutoff filter, $\bar{\bar{s}} = \bar{s}$, which is not true in general. The transfer function of the digital filter can be made to more closely approximate the spectral ideal at the computational expense of including more and more history (i.e., by using larger and larger values of m and n.)

Experimentation with prototype second- and fourth-order temporal filters lead to the fortuitous result that (for reasons to be addressed shortly) second-order filters have some inherent advantages and require relatively little storage. Consequently, attention was focused on second-order filters. The transfer function of our prototype filter is that shown in Fig. 1. By a simple

transformation, we modify the prototype filter to allow tuning of the cutoff frequency. The tuning parameter is R_c, which relates the actual (Ω_c) and prototypical (Ω'_c) cutoff frequencies as follows:

$$R_c = \frac{\Omega_c}{\Omega'_c} \tag{3}$$

Figure 2 compares an (artificially generated) raw time trace with its corresponding filtered trace for several values of the cutoff parameter R_c.

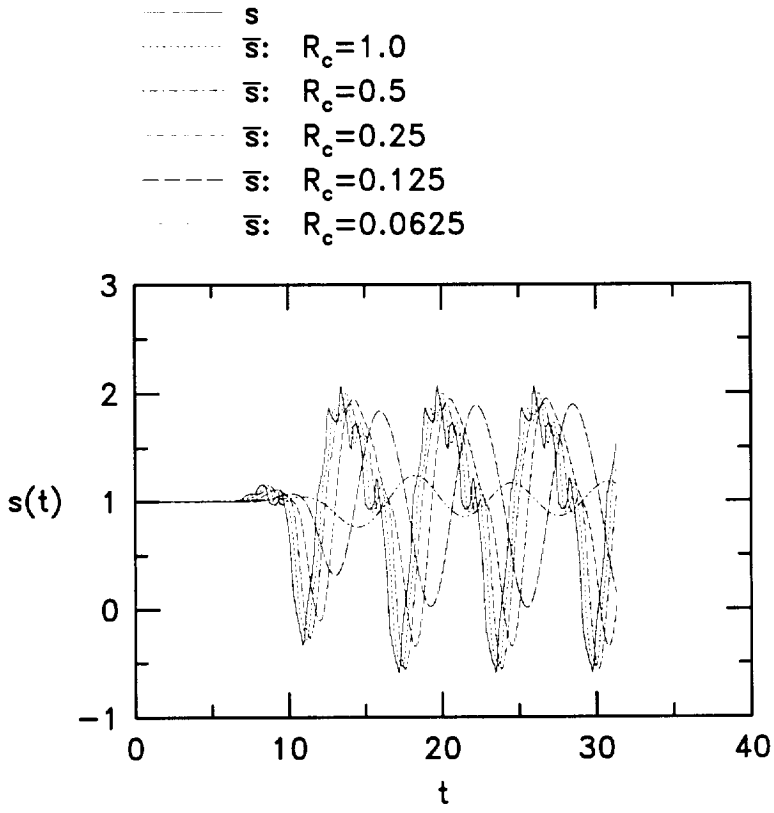

Filtered vs. unfiltered discrete time traces for selected values of cutoff frequency ratio R_c. Signal is periodic, with initial ramp function. Sample rate is 64 per period.

PRELIMINARY NUMERICAL TESTS: As a demonstration of the capability of the baseline LES algorithm, we simulated the evolution of a heated axisymmetric jet at Mach 0.8 and Reynolds number 10,000. A second-order causal Butterworth filter with $R_c = .125$ (as discussed above) was exploited for the LES. The results obtained were presented at the 3rd Symposium on Transitional and Turbulent Compressible Flows, Summer FED Meeting of the ASME, held in Vancouver in June 1997. The conference paper is attached in the Appendix. Following Colonius [2], we computed the compressible dilatation of the flow, which is shown in Fig. 5 of the paper. In terms of the dilatation, each large vortex appears as a quadrupole, which suggests that the large coherent structures may be the dominant acoustic sources (although this has yet to be confirmed).

Whereas a DNS calculation (not shown, for which 1280×512 grid points were needed) required 40 CPU hours, the 432×192 LES calculation required less than two CPU hours. Relative to DNS results, the shear-layer roll-up and pairing events were somewhat retarded, which suggested that the SGS model was overly dissipative, as expected. It was concluded that a dynamic SGS model would be beneficial in this context by limiting SGS dissipation to regions where the flow is inadequately resolved.

Fig. 6 of the paper presents the principal component of the resolved turbulent stress tensor $\mathcal{L}_{ij}$, computed by real-time temporal filtering of the resolved scales. In an LES computation, the magnitude of the terms of this tensor can be viewed as a measure of ill-resolution, or conversely, as identifying the locations where additional dissipation is needed to prevent numerical instability. That the components of the resolved turbulent stress tensor are both well-defined and smooth gave confidence that a dynamic procedure could be developed based on a temporal filter. This is the subject of the next section.

DYNAMIC MODELING: Having tested the candidate filter in LES, we re-directed attention to the development of a dynamic subgrid-scale model that exploits time-domain filtering. This effort was only partially successful. However, the reasons for the lack of complete success have to do more with perceived problems with the conventional practice of dynamic modeling, in general, than with the specifics of the temporal filter. A brief review of the

development of dynamic modeling is in order.

In the early 1990's, LES experienced a resurgence of interest, in large part due to the advent of dynamic SGS modeling (Germano et al. [5]), and it was quickly recognized that many of the shortcomings of LES could be addressed by dynamic models. The theoretical advantages of dynamic SGS models are now well established (Moin and Jimenez [14]; namely, the model coefficient is local, it is computed rather than prescribed, the model is applicable to transitional flow, and no near-wall damping is needed. Historically, dynamic modeling is rooted in the Germano [6] identity, which relates tensors obtained by filtering at two different scales. One of the terms in the Germano identity is the resolved turbulent stress tensor, $\mathcal{L}_{ij}$ (mentioned previously), which is a computible quantity. Unfortunately, dynamic modeling encounters certain practical difficulties, which are now also well known. A difficulty of physical origin arises when the model coefficient becomes locally negative due to a reverse cascade of energy (backscatter), in which case computations may "blow up" due to negative eddy viscosity. A second difficulty is numerical ill-conditioning inherent in the computed model constant. As a result, the model coefficient tends to oscillate wildly. Both problems are commonly addressed by *ad hoc* averaging of the computed coefficient over homogeneous spatial dimensions, a practice that unfortunately removes some of the local variation of the coefficient that lead to the desirability of dynamic SGS modeling in the first place.

Recently, considerable attention has been focused to address the problems of dynamic SGS models. Specifically, Ghosal et al. [7] have proposed mathematically elegant and rigorous dynamic modeling approaches based on variational formulations. Alternately, Meneveau et al. [13] developed a Lagrangian dynamic model in which smoothing of the model constant occurs in the time domain. This idea was recently extended to mixed models by Wu and Squires [25].

In general, most of these proposed fixes to the shortcomings of dynamic SGS models have gravitated toward greater and greater complexity and computational overhead. (One of the notable exceptions is the localized dynamic model of Piomelli and Liu [16], in which the model is approximated to arbitrary order). In the opinion of the PI, dynamic SGS modeling will realize its

potential in the simulation of flows of engineering interest if and only if its complexity and computational overhead are reduced significantly, and the continued pursuance of either *ad hoc* or inefficient fixes for dynamic models is ultimately counterproductive. What is needed is a simplified dynamic procedure.

The attempt to simplify the dynamic modeling procedure lead to to the idea of approximating the action of the filter by its Taylor-series expansion in terms of the filter parameter. The Taylor expansion was then used to approximate both the SGS stress tensor τ_{ij} and the resolved turbulent stress tensor $\mathcal{L}_{ij}$. Although, for simplicity, these (one-dimensional) expansions were initially carried out for time-domain filters, multidimensional Taylor expansions could be carried out (and have been carried out by other researchers; e.g., Horiuti [8]) for spatial filters as well. This simple approach has lead to a number of surprising and somewhat controversial revelations, which were documented in a conference paper presented at the First AFOSR Conference on DNS/LES, Ruston, LA, August, 1997. The paper is also attached in the Appendix. We summarize the most important findings below.

RESULTS: First, for LES, the filter, the SGS model, and the numerical method must be mutually consistent. Although this issue was partially addressed by Piomelli et al. in 1988 [15], it is not commonly recognized within the LES community even today. To be specific, present results show the Smagorinsky eddy-viscosity model to be consistent only with first- or second-order filters and inconsistent, for example, with spectral filters. Furthermore, there can be no universal Smagorinsky constant; the value depends on the properties of the filter. More importantly, it appears that, under certain conditions, the SGS stresses can be *directly approximated* (rather than *modeled*) by the computed resolved turbulent stresses without appealing to the Germano identity. The approximation error appears to small when the filter is of second order and the ratio of grid to test filter widths is unity, an unconventional practice. Direct approximation of the SGS stresses would avoid most or all the problems associated with conventional dynamic models.

Initially, these revelations were so surprising that the PI himself questioned their legitimacy. Gradually, evidence has accumulated to support present conclusions. Most convincing are the experimental results obtained

by Liu et al. [12] who investigated a turbulent jet by two-dimensional particle velocimetry. Liu et al. found high correlations between τ_{ij} and $\mathcal{L}_{ij}$ when filtering was accomplished consistently with either Gaussian or physical-domain top-hat filters (both of which are of low order in our terminology). On the other hand, negligible correlations existed when a sharp cut-off filter was used in Fourier space (i.e., a spectral filter in our terminology). Moreover, exact SGS stresses correlated relatively poorly with the Smagorinsky model. Recently, we conducted *a priori* tests based on highly resolved DNS results to compare exact SGS stress and resolved turbulent stress tensors. Extremely high correlations were obtained, for both temporal and spatial filters, although some phase error was incurred for temporal filters. Because of insufficient computational resources, these numerical tests considered only axisymmetric jet flow, and thorough validation must await the simulation of fully three-dimensional flows.

Results obtained by this PI, and corroborating results of other researchers to date, suggest that a simple, accurate, and efficient dynamic SGS model for LES, which would be applicable to aeroacoustics, is within reach. However, a number of fundamental unresolved issues need to be addressed. These are discussed in the next section.

2 Objectives of Proposed Future Work

The efforts of the past year have revealed a number of unresolved issues relative to LES, in general, and temporally filtered LES, in particular. An overarching consideration is the establishment of criteria that, when followed, guarantee filter/model/numerical-method consistency in the practice of LES. A second issue concerns the convergence of Taylor-series expansions of filter operators in the context of LES. A third issue, intimated by Speziale [22], concerns the Galilean invariance of SGS models that exploit temporal filters. And a fourth issue involves bounding the unavoidable phase errors inherent with causal temporal filters. The following objectives are proposed to address these issues.

1. Perform *a priori* tests based on DNS of three-dimensional decaying

isotropic turbulence to verify that the SGS stress tensor τ_{ij} can be directly approximated to suitable accuracy by the residual stress tensor $\mathcal{L}_{ij}$. Due to the unavailability of sufficient supercomputer time, this configuration is proposed in *lieu* of the DNS of a three-dimensional turbulent jet originally envisioned, which is estimated to require in excess of 400 Cray C90 hours. In contrast, the computation of isotropic turbulence can be accomplished in a very few CPU hours with an existing code that exploits fully spectral numerical methods.

2. If item 1 above is successful, then direct approximation, rather than modeling, of SGS stresses is virtually confirmed as a viable LES approach, given the already existing corroborating experimental evidence. Further mathematical attention should then be devoted to the convergence properties of the Taylor-expansion representations of the SGS and resolved turbulent stress tensors, to establish practical criteria for LES that guarantee the accuracy of this approximation. Based on preliminary results, such criteria are likely to involve the order of the filter, the ratio of the grid and test filter widths r, and the dimensionless filter cutoff Ω_c.

3. The mathematical analysis performed above, which examines filter-model consistency, should be expanded to include consistency with the numerical scheme, and a set of criteria for fully self-consistent LES should be established. These criteria will be codified into a set of practical guidelines for the practitioners of LES.

4. Speziale [22] has given examples of SGS models based on spatial filters and in common usage that fail the test of Galilean invariance. A later paper [23] suggests that time-domain filters may predispose SGS models to violations of Galilean invariance. This issue is poorly understood within the LES community, and we propose to examine the issue afresh. Recently, Meneveau et al. [13] have proposed a dynamic model that exploits time-domain filtering in a Lagrangian frame of reference to preserve Galilean invariance. However, it is not yet clear if the Lagrangian frame is a necessity.

5. Investigate the seriousness of the inherent phase-lag errors associated with causal temporal filters and attempt to establish practical bounds

for such errors.

6. Based on resolution of the items above, recommend and/or propose a SGS model applicable to aeroacoustics and conduct a validation-of-concept test for axisymmetric-jet flow. The recommendation will include an assessment of the practicality of time-domain filtering for LES.

References

[1] A. A. Aldama, *Filtering Techniques for Turbulent Flow Simulation*, Springer-Verlag, Berlin, 1990.

[2] T. Colonius, S.K. Lele, and P. Moin, "The Sound Generated by a Two-Dimensional Shear Layer: A Comparison of Direct Computations and Acoustic Analogies," CEAS/AIAA Paper No. 95-036, 1995.

[3] Y.M. Dakhoul and K.W. Bedford, "Improved Averaging Method for Turbulent Flow Simulation. Part I: Theoretical Development and Application to Burger's Transport Equation," *Int. J. Numer. Meth. Fluids*, Vol. 6, 1986, pp. 49-64.

[4] G. Erlebacher, M. Y. Hussaini, C. G. Speziale, and T. A. Zang, "Toward the Large-Eddy Simulation of Compressible Turbulent Flows," *J. Fluid Mech.*, Vol. 238, 1992, pp. 155-185.

[5] M. Germano, U. Piomelli, P. Moin, and W. Cabot, "A Dynamic Subgrid-Scale Eddy-Viscosity Model," *Phys. Fluids A*, Vol. 3, No. 7, 1991, p. 1760.

[6] M. Germano, "Turbulence: The Filtering Approach," *J. Fluid Mech.*, Vol. 238, 1992, pp. 325-336.

[7] S. Ghosal, T. S. Lund, P. Moin, and K. Akselvoll, "A Dynamic Localization Model for Large-Eddy Simulation of Turbulent Flows," *J. Fluid Mech.*, Vol. 286, 1995, pp. 229-255.

[8] K. Horiuti, "A New Dynamic Two-Parameter Mixed Model for Large-Eddy Simulation," *Phys. Fluids A*, 1997 (to appear).

[9] S. K. Lele, "Compact Finite Difference Schemes with Spectral-Like Resolution," *J. Comput. Phys.*, Vol. 103, 1992, pp. 16-42.

[10] M.J. Lighthill, "On Sound Generated Aerodynamically: 1. General Theory," *Proc. Roy. Soc. (A)*, Vol. 211, No. 1107, 1952, pp. 564-587.

[11] G.M. Lilley, "Aerodynamic Noise Theory," unpublished ICASE Report, 1993.

[12] S. Liu, C. Meneveau, and J. Katz, "On the Properties of Similarity Subgrid-Scale Models as Deduced from Measurements in a Turbulent Jet," *J. Fluid Mech.*, Vol. 275, No. 83, 1994, pp. 83-119.

[13] C. Meneveau, T. S. Lund, and W. H. Cabot, "A Lagrangian Dynamic Subgrid-Scale Model of Turbulence," *J. Fluid Mech.*, 1997, to appear.

[14] P. Moin and J. Jimenez, "Large-Eddy Simulation of Complex Turbulent Flows," AIAA Paper No. 93-3099, 1993.

[15] U. Piomelli, P. Moin, and J. H. Ferziger, "Model Consistency in Large-Eddy Simulation of Turbulent Channel Flow," *Phys. Fluids A*, Vol. 31, No. 7, 1988, pp. 1884-1891.

[16] U. Piomelli and J. Liu, "Large-Eddy Simulation of Rotating Channel Flows Using a Localized Dynamic Model," *Phys. Fluids A*, Vol. 7, No. 4, 1995, pp. 839-848.

[17] W.H. Press, B.P. Flanner, S.A. Teukolsky, W.T. Vetterling, *Numerical Recipes: The Art of Scientific Computing*, Cambridge University Press, Cambridge, 1986.

[18] C.D. Pruett, T.A. Zang, C.-L. Chang, and M.H. Carpenter, "Spatial Direct Numerical Simulation of High-Speed Boundary-Layer Flows–Part I: Algorithmic Considerations and Validation," it Theoret. Comput. Fluid Dynamics, Vol. 7, No. 1, 1995, pp. 49-76.

[19] C.D. Pruett, "A Semi-Implicit Method for Internal Boundary Layers in Compressible Flows," *Comp. Meth. Applied Mech. Eng.*, Vol. 137, 1996, pp. 379-393.

[20] C.D. Pruett, "Time-Domain Filtering for Spatial Large-Eddy Simulation," presented at the 3rd Symposium on Transitional and Turbulent Compressible Flows, 1997 ASME Fluids Engineering Division Summer Meeting, June 22-26, 1997.

[21] C.D. Pruett, "Toward Simplification of Dynamic Subgrid-Scale Models," presented at the First AFOSR Conference on DNS and LES, Ruston, LA, Aug. 3-8, 1997.

[22] C. G. Speziale, "Galilean Invariance of Subgrid-Scale Stress Models in the Large-Eddy Simulation of Turbulence," *J. Fluid Mech.*, Vol. 156, 1985, pp. 55-62.

[23] C. G. Speziale, "On the Decomposition of Turbulent Flow Fields for the Analysis of Coherent Structures," *Acta Mechanica*, Vol. 70, 1987, pp. 243-250.

[24] R. D. Strum and D. E. Kirk, *First Principles of Discrete Systems and Digital Signal Processing*, Addison-Wesley, New York, 1988.

[25] X. Wu and K. D. Squires, "Large-Eddy Simulation of an EquilibriumThree-Dimensional Turbulent Boundary Layer," *AIAA J.*, (to appear).

Appendices: Papers Related to Previous and Proposed Grant Work

TIME-DOMAIN FILTERING FOR SPATIAL LARGE-EDDY SIMULATION

C. David Pruett*
Department of Mathematics
James Madison University
Harrisonburg, Virginia 22807 USA
540-568-6227 (T) 540-568-6857 (F) dpruett@math.jmu.edu

1997 ASME Fluids Engineering Division Summer Meeting
FEDSM'97 June 22-26, 1997

FEDSM97-3117

ABSTRACT

An approach to large-eddy simulation (LES) is developed whose subgrid-scale model incorporates filtering in the time domain, in contrast to conventional approaches, which exploit spatial filtering. The method is demonstrated in the simulation of a heated, compressible, axisymmetric jet, and results are compared with those obtained from fully resolved direct numerical simulation. The present approach was, in fact, motivated by the jet-flow problem and the desire to manipulate the flow by localized (point) sources for the purposes of noise suppression. Time-domain filtering appears to be more consistent with the modeling of point sources; moreover, time-domain filtering may resolve some fundamental inconsistencies associated with conventional space-filtered LES approaches.

1 INTRODUCTION

By definition, direct numerical simulation (DNS) is the numerical solution of the Navier-Stokes equations without recourse to empirical models. In concept, the fluid motions are resolved down to the Kolmogorov length scale, at which eddies succumb to viscous dissipation. Consequently, for high Reynolds number flow, the computational requirements of fully resolved DNS are staggering.

In contrast, in large-eddy simulation (LES), the large scales of motion are resolved in space and time on a suitable computational grid; however, the effects of the subgrid-scale motions on the evolution of the large scales are modeled. Relative to DNS, LES is conducted on relatively coarse grids at reasonable computational expense. In practice, LES involves filtering the Navier-Stokes equations in space or time or both. The filtered equations of motion contain subgrid-scale (residual) stress terms whose effects must be modeled.

Both DNS and LES can be classified fundamentally as temporally or spatially evolving. The distinction between temporal and spatial approaches is muddied by most applications of LES. In particular, nearly all current LES approaches, *whether temporal or spatial*, exploit spatial filtering. In their review paper, Moin and Jimenez (1993) state: "Historically, temporal filtering has not been used," one presumes for reasons of computational efficiency. However, because the roles of space and time are fundamentally interchanged in temporal vs. spatial simulations, we suggest that spatial filtering is more appropriate for temporal LES, and conversely, temporal filtering is more appropriate for spatial LES. Indeed, time-domain filtering may remove some of the conceptual and practical inconsistencies that have been observed by practitioners of LES, a few of which are discussed briefly below.

First, as intimated by Germano (1992), LES can be viewed as lying somewhere near the middle of a spectrum of numerical solution techniques with DNS at one end and Reynolds-averaged Navier-Stokes (RANS) at the other end. In our opinion, this point of view is most self-consistent if time-domain filtering is exploited in LES as it is in RANS. Second, Moin and Jimenez (1993) observe that the operations of filtering and differentiation do not commute on a non-uniform mesh. Consequently, most subgrid-scale models inadvertently impose different levels of dissipation in different regions of the computational domain, a problem made worse on the highly stretched grids associated with complicated geometries. This problem should be circumvented by temporal filtering in conjunction with uniform time increments. Third, again according to Moin and Jimenez (1993): "In LES, it is highly desirable for the filter width to be significantly larger than the computational mesh to separate the numerical and modeling errors. Practical considerations, however, usually require the filter width and mesh to be of the same order. In this case, there does not appear to be a necessity for higher than second order numerical methods for LES." In contrast, for the present temporally filtered approach, the filter width is typically an order of magnitude larger than the time step. Fourth, it may be desirable in spatial DNS or LES of certain physical problems (e.g., jet flow) to allow for time-dependent localized (point) sources as a means of manipulating the flow for the purposes of control. For example, such sources could be used to introduce local disturbances to enhance or inhibit mixing. Dakhoul and Bedford (1986) suggest that spatial filtering is fundamentally inconsistent with the introduction of point sources, whereas temporal filtering of a point source is

*Research conducted under NASA Grant NAS1-1802, monitored by Dr. Kristine R. Meadows, NASA Langley Research Center, Hampton, VA 23681-0001

well defined.

Whereas Dakhoul and Bedford (1986) and Aldama (1990) propose and develop space-time filters for LES, the author is unaware of any purely time-filtered approach. In the next few sections, we develop and demonstrate a spatial LES concept based on filtering in the time domain, and we apply the approach to the investigation of large coherent structures (CS) in a heated subsonic axisymmetric jet. For several reasons, the jet-flow problem is well suited to the particular LES approach. First, free shear layers, jets, and wakes, whose mean streamwise velocity profiles are inflectional, are inviscidly unstable to disturbances of a broad spectrum of frequencies (wavelengths). As a consequence, DNS of three-dimensional (3D) unbounded shear flows is presently impractical because of the extremely fine grid resolution required, and some sort of subgrid-scale dissipation is virtually a necessity. Second, the problem is of immediate practical interest to the field of computational aeroacoustics (CAA). Specifically, it is generally believed that, for supersonic jets, most of the noise originates from the CS rather than from the small-scale turbulence (Seiner, 1984, and Tam, 1995). For subsonic jets, the origin of noise is less certain. In his recent review paper, Tam (1995) expresses the view that subsonic jet noise originates primarily from fine-scale turbulence. Our results (preliminary at the present time) would suggest otherwise. Thus, spatial LES may provide a tool by which to investigate the physics of noise production and suppression in jets. Last, because no walls are present, we avoid for the time being the difficulties experienced by many subgrid-scale models in the vicinity of solid boundaries.

In the next section, time-domain filtering is discussed in general, and a prototype causal digital filter is developed. The governing equations for DNS are discussed in Section 3, and the equations are modified for LES based on adaptation of the so-called SEZHu ("says who") model of Speziale and coworkers (1988). The present model differs from the SEZHu model in that it exploits temporal rather than spatial filtering. The axisymmetric-jet test case is defined in Section 4. The numerical approach to the solution of the governing equations, adapted from Pruett et al. (1995), is addressed briefly in Section 5. Results of LES for the axisymmetric-jet problem are presented in Section 6 and are compared with well-resolved DNS results. Finally, some brief conclusions are offered in Section 7.

2 CAUSAL FILTERING

Time-domain filters fall into either of two categories: causal or acausal. For application to LES, only causal filtering is realizable. By definition, causal temporal filters exploit present and past information only, the future being inaccessible. Consequently, in this section, we consider prototypical continuous and discrete causal filters. A continuous filter is presented for conceptual purposes; an analogous discrete filter is exploited in practice.

A CONTINUOUS CAUSAL FILTER: If $s(t)$ represents a smooth continuous signal in time t, then a continuous low-pass causal filter can be constructed simply by integrating the signal over the interval Δ, the temporal window width, as follows:

$$\overline{s}(t,\Delta) = \frac{1}{\Delta}\int_{t-\Delta}^{t} s(\tau)d\tau \tag{1}$$

The input to Eq. 1 is the raw signal $s(t)$, and the output is the continuous filtered signal, denoted by $\overline{s}(t,\Delta)$. From elementary calculus, the following property of the filter defined by Eq. 1 is readily derived:

$$\overline{s}(t,0) \equiv \lim_{\Delta\to 0}\overline{s}(t,\Delta) = s(t) \tag{2}$$

In general, $\overline{\overline{s}} \neq \overline{s}$ If Δ represents some moderately large temporal window, then filtering $s(t)$ via Eq. 1 will tend to remove oscillations of high frequency relative to Δ while preserving low-frequency oscillations, which defines a "low-pass" time-domain filter.

LINEAR DIGITAL CAUSAL FILTERS: Let us digitize the continuous signal $s(t)$ such that $s_i = s(t_i)$, where $t_i = i\Delta t$, and Δt is the (constant) time interval between samples. Typically, for applications to LES, Δ should be an order of magnitude larger than Δt. The approximation of Eq. 1 by a linear quadrature rule results in its discrete analog

$$\overline{s}_i = \sum_{j=0}^{m} p_j s_{i-j} \tag{3}$$

where the filter coefficients p_j are determined to give the filter certain desirable properties (e.g., low-pass characteristics, stability, and high-order accuracy at low frequencies). Following Press et al. (1986), we generalize the linear digital filter given in Eq. 3 to allow the use of previously filtered data. Specifically, suppose

$$\overline{s}_i = \sum_{j=0}^{m} p_j s_{i-j} + \sum_{k=1}^{n} q_k \overline{s}_{i-k} \tag{4}$$

The filter of Eq. 4 is "nonrecursive" if $q_k = 0$ for all k and "recursive" if, for at least one k, $q_k \neq 0$, in which case the current value of the filtered quantity is a linear combination of previous unfiltered and filtered values.

FREQUENCY RESPONSE: It is instructive to examine the frequency response of the filter associated with Eq. 4. From Press et al. (1986), the transfer function, which quantifies the frequency response, is given by

$$H(\Omega) = \frac{\sum_{j=0}^{m} p_j e^{-\imath j\Omega}}{1 - \sum_{k=1}^{n} q_k e^{-\imath k\Omega}} \tag{5}$$

where $\imath = \sqrt{-1}$, $\Omega = \omega^*\Delta t^*$ is the dimensionless frequency, $\omega^* = 2\pi f^*$ is the dimensional circular frequency, and f^* is the dimensional physical frequency. (Throughout this work, we denote dimensional quantities by asterisks.) In general, the frequency response of a recursive filter is related to a rational polynomial function in the complex variable $1/\zeta$, where $\zeta = e^{\imath\Omega}$. Thus, recursive filters are to nonrecursive filters what compact-difference operators are to standard finite-difference operators. The rational polynomial form of the transfer function allows considerable latitude in shaping the frequency response. Fig. 7 compares the modulus of the transfer function of a prototypical low-pass digital recursive filter with that of an idealized "spectral cutoff" filter, for a nominal cutoff frequency Ω_c'. Note that, for the spectral cutoff filter, $\overline{\overline{s}} = \overline{s}$, which, as we have mentioned previously, is not true in general. The transfer function of the digital filter can be made to more closely approximate the spectral ideal at the expense

of including more and more history (i.e., by using larger and larger values of m and n.)

For the purposes of time-filtered LES, the design constraints for the discrete filter are: 1) stability for all t_i; 2) $H(0) = 1$; 3) high-order accuracy; 4) $|H(\Omega)| = 0$ for $\Omega > \Omega_c$; and 5) as little storage required as possible. For reasons to be addressed fully in a subsequent paper, one is lead to the fortunate if surprising conclusion that second-order filters are optimal for the present application to LES. First, second-order causal filters require relatively little storage for history. Second, to avoid mixing the truncation errors of the filter and numerical method, one should invoke a filter with no higher order than that of the time-advancement scheme. Thus, a second-order filter is compatible with the present third-order time advancement scheme (see Section 5). Third, and a subtle point, it can be shown that second-order filtering is consistent with the underlying subgrid-scale model (Pruett, 1996b). Consequently, for our purposes, we have followed the design procedures outlined in the digital signal filtering text by Strum and Kirk (1988). Formally, our prototype filter is a second-order, impulse-invariant, digital Butterworth low-pass filter, for which $m = n = 2$, and $p_0 = 0$. Technically, Butterworth filters are "all-pole" filters, whose transfer functions are maximally flat in the vicinity of the origin. Unfortunately, however, the transfer functions of Butterworth filters do not vanish identically for large values of Ω. In practice, this is not a problem as will be shown subsequently. The nominal cutoff frequency for our prototype filter is $\Omega_c' = 1.0$, for which $|H(\Omega_c')|^2 = 0.5$.

A suitable generalization from the prototype filter to a tunable-cutoff low-pass filter is made by incorporating a parameter R_c, defined as the ratio of the actual and prototypical cutoff frequencies, namely

$$R_c = \frac{\Omega_c}{\Omega_c'} = \frac{\Delta t}{\Delta} \tag{6}$$

Note that $R_c \to 0$ for the discrete filter is analogous to $\Delta \to \infty$ for the continuous filter of Eq. 1. Conversely, as $R_c \to \infty$, $\Delta \to 0$, in which case $\overline{s}(t, \Delta) \to s(t)$ by the property of Eq. 2. Fig. 7 shows the frequency response of the present filter for $R_c = .125$, a value typical for the current time-filtered LES approach. Note that high-frequency oscillations are virtually eliminated by the present filter, as desired.

3 GOVERNING EQUATIONS

We first specify the governing equations for DNS and then present the governing system as modified for LES.

DNS: As a basis on which to evaluate various LES solutions, we require a well-resolved DNS solution for the axisymmetric-jet problem. For a compressible fluid, it is appropriate to define a fluid state vector $[\rho, p, T, u, v, w]^T$ comprised of the density ρ, pressure p, temperature T and velocity components u, v, and w. The governing equations for the axisymmetric-jet problem are adapted from those presented in Pruett et al. (1995) for a body-fitted coordinate system $\vec{x} = [x, \theta, z]^T$ on an axisymmetric body, where x as the arc length along the body, θ is the azimuthal angle, z is the coordinate normal to the body, $r = R + z\cos\phi$ is the radial coordinate, $R(x)$ is the body radius, and $\phi(x)$ is the angle of the surface tangent to the body. For the jet-flow application, $R = \phi = 0$, in which case the coordinate system degenerates to $z = r$ with x as the axial coordinate, whereby u and w become the axial and radial velocities, respectively. Because $R = 0$, the equations are geometrically singular along the jet axis. For the continuity equation, the singularity is removed by applying L'Hopital's rule along the axis ($z = 0$). The singularity is not problematic for the momentum and energy equations because axial boundary conditions replace the governing equations along the axis. Specifically, considerations of symmetry require that the azimuthal velocity (v) vanish everywhere and that

$$\frac{\partial T}{\partial z} = \frac{\partial u}{\partial z} = w = 0 \quad (z = 0) \tag{7}$$

LES AND SUBGRID-SCALE MODEL: If the compressible Navier-Stokes equations (CNSE) are filtered in the time domain according to Eq. 1, the resulting equation system is formally identical to that of Eqs. (15), (16), and (34) of Erlebacher et al. (1992), where overbars and tildes distinguish conventionally filtered and Favre-filtered quantities, respectively. In general, the use of Favre-filtered (density-weighted) variables reduces the complexity of the filtered CNSE. Specifically, for example, the Favre-filtered axial velocity is defined as

$$\tilde{u} = \frac{\overline{\rho u}}{\overline{\rho}} \quad (\text{or} \quad \overline{\rho}\tilde{u} = \overline{\rho u}) \tag{8}$$

Other Favre-filtered quantities are defined analogously. For the filtered equations, the fluid state vector is comprised of a mixture of conventionally and Favre-filtered quantities, namely $[\overline{\rho}, \overline{p}, \tilde{T}, \tilde{u}, \tilde{v}, \tilde{w}]^T$. The filtered governing equations contain residual stresses not present in the original equations, which are decomposed into Leonard-stress, cross-stress, and Reynolds-stress terms denoted by $\mathbf{L}$, $\mathbf{C}$, and $\mathbf{R}$, respectively, following the notation of Erlebacher et al. (1992). Of these, $\mathbf{C}$ and $\mathbf{R}$ must be modeled; $\mathbf{L}$ can be computed.

Several candidate subgrid-scale models are available; however, for our present purpose, we adapt the SEZHu model (Speziale et. al. 1988) as adapted by Erlebacher et al. (1992). Several considerations favor this selection. First, to demonstrate the time-filtered approach, the filtering process must participate in the model, rather than simply serving as a conceptual framework as it does in some models (e.g., Smagorinsky). Second, although present results suggest that a dynamic model (Germano et al., 1991) is desirable, we wanted initially to avoid some of the pitfalls of dynamic subgrid-scale models, particularly, the need to smooth the computed model constants. Finally, the SEZHu model is extremely well documented in Erlebacher et al. (1992).

Formally, our implementation of the SEZHu model is virtually identical to that of Erlebacher et al. (1992), except, of course, that the filter is temporal. In tensor notation, the dimensionless filtered equations, with the modeled terms denoted by underlines, are

$$\gamma M^2 \overline{p} = \overline{\rho}\tilde{T} \tag{9}$$

$$\frac{\partial \overline{\rho}}{\partial t} + \frac{\partial(\overline{\rho}\tilde{u}_k)}{\partial x_k} = 0 \tag{10}$$

$$\frac{\partial(\overline{\rho}\tilde{u}_k)}{\partial t} + \frac{\partial}{\partial x_l}\left[\overline{\rho}\tilde{u}_k\tilde{u}_l + \underline{\overline{\rho}(\widetilde{u_k u_l} - \tilde{u}_k\tilde{u}_l)}\right] = -\frac{\partial \overline{p}}{\partial x_k} + \frac{\partial}{\partial x_l}\left[(\mu_v + \underline{\mu_T})\tilde{S}_{kl}\right] \tag{11}$$

$$\frac{\partial \overline{\rho}}{\partial t} + \frac{\partial}{\partial x_k}\left[\overline{\rho}\tilde{u}_k + \underline{\frac{\overline{\rho}}{\gamma M^2}(\widetilde{u_k T} - \tilde{u}_k \tilde{T})}\right] =$$

$$-(\gamma-1)\overline{p}D + \frac{\partial}{\partial x_k}\left[(\kappa_v + \underline{\kappa_T})\frac{\partial \tilde{T}}{\partial x_k}\right] + \frac{(\gamma-1)}{Re}\overline{\Phi} \qquad (12)$$

where

$$D = \frac{\partial \tilde{u}_k}{\partial x_k} \qquad (13)$$

is the resolved-scale dilatation,

$$\tilde{S}_{kl} = 2(\tilde{e}_{kl} - \frac{1}{3}D\delta_{kl}) \qquad (14)$$

δ_{kl} is the kronecker delta, and $\tilde{e}_{kl}$ is the resolved-scale strain-rate tensor, namely

$$\tilde{e}_{kl} = \frac{1}{2}\left[\frac{\partial \tilde{u}_k}{\partial x_l} + \frac{\partial \tilde{u}_l}{\partial x_k}\right] \qquad (15)$$

For brevity, the physical viscosity and thermal conductivity are denoted, respectively, as

$$\mu_v = \frac{\tilde{\mu}}{Re} \quad : \quad \kappa_v = \frac{\tilde{\mu}}{M^2 Re Pr} \qquad (16)$$

where Re, Pr, and M are the dimensionless Reynolds, Prandtl, and Mach numbers, respectively. Similarly, the eddy viscosity and the eddy thermal conductivity are given by

$$\mu_T = C_r l^2 \overline{\rho}\Pi^{1/2} \quad : \quad \kappa_T = \frac{\mu_T}{\gamma M^2 Pr_T} \qquad (17)$$

where l is a length scale to be defined shortly, Pr_T is the turbulent Prandtl number, γ is the ratio of specific heats, and

$$\Pi = \tilde{S}_{kl}\tilde{S}_{kl} \qquad (18)$$

Whereas the underlined terms on the right-hand sides of the governing equations model **R**, the underlined terms on the left-hand sides, which are properly referred to as the resolved stresses, are computible by filtering the resolved fields. For the present subgrid-scale model, the resolved stresses model the sum $\mathbf{L} + \mathbf{C}$.

In the original SEZHu subgrid-scale model (Speziale et al., 1988), the Reynolds stresses were split into deviatoric and isotropic parts, which were modeled separately. In the more detailed paper of Erlebacher et al. (1992), on which the present approach is based, the isotropic part is disregarded on the rationale that its contribution should be small for turbulent Mach numbers $M_t < 0.6$ (a constraint satisfied by most compressible flows). Several other subtleties of the implementation of the model are not immediately apparent upon the study of Erlebacher et al. (1992). First, the viscous-stress terms of the filtered momentum equations, and the dissipation function Φ and thermal-stress terms of the filtered energy equation, formally involve conventionally filtered rather than Favre-filtered quantities. Because these quantities are unavailable, however, they are approximated by their Favre-filtered equivalents. Second, terms that arise from subgrid-scale fluctuations of μ_v and κ_v are neglected. Third, the resolved stresses are computed using $\overline{\rho}$ rather than ρ, the latter of which is unavailable. These approximations should be considered as additional modeling errors.

MODEL CONSTANTS: Equation 17 requires values for three constants. Following Erlebacher et al. (1992), we use $Pr_T = 0.5$ and $C_r = 0.012$. It remains to determine l, which, for the original SEZHu model, is a characteristic length scale related to spatial grid resolution. Specifically, Erlebacher et al. (1992) show that $l = c\Delta x$ is optimal (in the sense of preserving the Galilean invariance of certain terms of the model) for $c = 2$, where Δx is the actual computational grid spacing.

Here, we must determine l based on the choice of the temporal scale Δ (or equivalently, R_c), for which purposes we appeal to results from the area of hydrodynamic stability. From linear stability theory, we know that jets, wakes, and free shear layers are dispersive; i.e., waves of different frequencies propagate at different phase velocities. However, disturbances of moderate to high frequencies propagate at a velocity approximately that of $U^*_{\rm av}$, the average of the jet and ambient velocities. Accordingly, we define Δx^* as the characteristic size of an eddy associated with a disturbance of cutoff frequency f_c^*; that is

$$\Delta x^* = \frac{U^*_{\rm av}}{f_c^*} = \frac{2\pi U^*_{\rm av}\Delta t^*}{R_c} \qquad (19)$$

Finally, we note that the CNSE are recovered from the governing equations in the limit as $\Delta \to 0$.

4 TEST CASE

The numerical test case was chosen to approximately replicate an acoustics experiment that is being conducted at NASA Langley Research Center. Specifically, we investigate a heated subsonic ($M = 0.8$) jet exhausting into a nearly quiescent atmosphere. The jet temperature T_j^*, on which the Mach number is based, is 600 F (1059.6 R), and the ambient temperature is 70 F (529.6 R). The nominal jet radius is $R_j^* = 0.5$ in. (0.0417 ft.). The ambient pressure in the physical experiment is approximately one atmosphere (2160 psf.). However, this results in too high a Reynolds number for a DNS computation of reasonable expense; consequently, the computational experiment assumes an ambient pressure 10 percent that of the physical experiment; that is, 216 psf, which results in $Re = 10153$ based on the jet conditions and the nominal jet radius. In the physical experiment, the ambient air was quiescent. However, computational experiments with unbounded shear layers typically encounter numerical difficulties (as did the present work) whenever the ambient stream is perfectly quiescent (Tannehill et al., 1984). Consequently, it is customary for the jet to exhaust into a coflowing stream with a velocity of a few percent of the jet velocity. For the present problem, we use an ambient to jet velocity (U_j^*) ratio of 10 percent. We further assume that the jet is fully expanded, in which case, in the absence of any disturbances, the pressure is constant both radially and axially.

In the governing equations and in the results to follow, all lengths have been normalized by R_j^*, and the velocities, temperature, and density, have been normalized by U_j^*, T_j^*, and ρ_j^*, respectively. Pressure is normalized by $\rho_j^* U_j^{*2}$.

5 NUMERICAL METHODOLOGY

Spatial DNS and LES can be viewed as three-step processes. First, an unperturbed time-independent base state is obtained, usually by boundary-layer techniques. Second, the base state is subjected to either random or temporally periodic perturbations, which are typically imposed at or near the computational inflow boundary. The structure of these disturbances is commonly obtained from linear stability theory, or more recently, from parabolized stability equation (PSE) methodology. Third, the spatial evolution of the propagating disturbances is computed by solution of the complete Navier-Stokes equations, with (LES) or without (DNS) subgrid-scale models. We discuss in turn each of these steps in the context of the current problem.

COMPUTATION OF THE BASE STATE: The application of standard fully implicit boundary-layer techniques to the axisymmetric jet revealed an unanticipated computational difficulty; namely, the Jacobian matrix associated with the iteration procedure was extremely ill-conditioned and the iteration did not converge. The computational problem arises from a reversal of sign in the transverse velocity experienced by internal boundary-layer flows such as jets, wakes, and free shear layers. To circumvent this numerical difficulty, a semi-implicit boundary-layer technique was developed, which is is documented in Pruett (1996a). The interested reader is referred to this paper for details. Also to avoid numerical difficulties, the internal shear layer is given finite thickness at the lip of the jet. The boundary-layer solution can be viewed as an unstable equilibrium state of the CNSE.

IMPOSITION OF THE DISTURBANCES: The nature of instabilities is different for wall-bounded and free-shear flows. Specifically, wall-bounded flows are subject to viscous instabilities, for which typically only a relatively narrow band of frequencies are unstable. In contrast, free-shear layers, jets, and wakes are subject to inviscid instabilities over a broad range of frequencies. Relative to viscous instabilities, inviscid instabilities experience rapid growth rates. Thus, for simulating instability waves in wall-bounded flows, it is essential that the imposed disturbances be consistent with eigenfunctions obtained from stability theory; otherwise, one introduces spatial transients that may corrupt the particular instability of interest. On the other hand, one can be somewhat cavalier in imposing disturbances in free-shear flows because of the flow's tendency to rapidly organize arbitrary disturbances into the dominant eigenmodes. Consequently, following Mankbadi et al. (1994), at the inflow boundary, we impose a temporally periodic fluctuation comprised of a few harmonics of specified frequencies, but whose structure is not derived from stability theory. At present, we impose the disturbance only through the streamwise velocity. Specifically, at the inflow boundary $x = x_0$

$$u(t, x_0, z) = u_B(x_0, z) + \epsilon u'(t, z) \quad (20)$$

$$u'(t, z) = \phi(z)\left[\sin(\omega_f t) + \cos(0.5\omega_f t)\right] \quad (21)$$

$$\phi(z) = \exp[-(2(z-1))^4] \quad (22)$$

where the subscript B denotes the base state, the prime denotes a fluctuating quantity, and the subscript f denotes the fundamental frequency. The function $\phi(z)$ is used to shape the disturbance profile so that the disturbance is largest near the edge of the jet but essentially vanishes along the jet axis and at the far-field boundary. Numerical experimentation reveals the most rapid development of the jet for $\omega_f = \pi$, which corresponds to a Strouhal number ($St = f_f^* R_j^*/U_j^*$) of 0.5, in keeping with the observations of Mankbadi et al. (1994). Following the early computational investigation of free-shear layers by Riley and Metcalfe (1980), we include an out-of-phase subharmonic component to enhance pairing of adjacent vortices. At present, we use a forcing amplitude of $\epsilon = 0.005$, which is ramped up slowly (over a time interval of one period of oscillation at the fundamental frequency) to minimize temporal transients.

DNS AND LES METHODOLOGIES: For both the DNS and LES, we adapt the high-order numerical scheme of Pruett et al. (1995), to which the reader is referred for details. Briefly, this algorithm exploits fully explicit time advancement, high-order compact-difference methods (Lele, 1992) for aperiodic spatial dimensions, and spectral collocation methods for periodic spatial dimensions. Specifically, for the present axisymmetric-jet application, we use fourth- and sixth-order compact difference schemes in the axial and radial dimensions, respectively. The azimuthal dimension, of course, does not come into play for the axisymmetric case. The method of Pruett et al. (1995) uses a variable step for time advancement in the context of a three-stage, low-storage Runge-Kutta (RK3) scheme. However, the present LES application, which involves temporal filtering, requires a constant time step. Consequently, the original Runge-Kutta temporal integration has been replaced by a fixed-length, multiple-step, third-order Adams-Bashforth (AB3) technique. An additional motivation for replacing the RK3 method was that it was not immediately clear to the author how temporal filtering would interact with time advancement whenever multiple stages per time step were involved, the fear being the possibility of numerical instability. The storage requirement for the algorithm with AB3 time advancement is about 150 percent that of the original algorithm with RK3. In general, multiple-step methods are not self starting. The AB3 integration is started initially with a single first-order Euler step followed by one second-order Adams-Bashforth step. Because the perturbation is ramped slowly to full amplitude, and the initial state is in (near) equilibrium, the initial loss of temporal accuracy is inconsequential.

For both the DNS and the LES, the symmetry conditions given by Eq. 7 are imposed along the jet axis. At the inflow boundary, for the present axisymmetric-jet problem, the flow is everywhere subsonic, and one characteristic points upstream. Consequently, not all flow variables can be specified. Currently, we specify v, w, T, and the incoming Riemann invariants. At the far-field boundary ($z = z_{\max}$), we adapt the non-reflecting boundary conditions of Thompson (1987) as modified by Pruett et al. (1995). At the outflow boundary, we exploit a buffer-domain approach (Streett and Macaraeg, 1989/1990). Near the outflow boundary, a buffer zone of finite width is constructed in which both the base state and the governing equations are modified to ensure that all waves propagate out of the domain.

Finally, we note that the present LES algorithm is one of few to incorporate high-order numerical methods, another being that of El-Hady and coworkers [5].

COMPUTATIONAL EFFICIENCY: *On the same grid*, an LES computation with the present algorithm requires not quite twice the computational effort as DNS and approximately 2.5 times the storage for 3D flows (twice the storage for two-dimensional or axisymmetric flows). Most of the additional memory is relegated to storage of the time histo-

ries of quantities associated with the time-filtered approach. One must keep in mind, however, that, by definition, LES allows computations on coarser grids than DNS. If, for the present LES algorithm, for example, the grid resolution relative to DNS could be reduced by a factor of three in each of the three spatial dimensions and time, then storage requirements would be diminished by a factor of approximately ten, and processor time would diminish by a factor of approximately 40. Thus, measures of efficiency in LES must consider not only nominal storage and operation counts, but also the potential grid-coarsening factor, which could conceivably be higher for temporally filtered LES than for conventional approaches.

6 RESULTS

For the DNS and LES results presented below, the computational domain was

$$0 \leq x \leq 20 \quad ; \quad 0 \leq z \leq 5 \tag{23}$$

The length of the domain was sufficient to allow one pairing of the adjacent vortices shed at the edge of the jet. The final 16 percent of the axial extent of the domain lies in the buffer domain; results within the buffer domain should be disregarded as unphysical. For convenience in presenting results, we define t_P, the time in periods of oscillation at the fundamental disturbance frequency.

DNS: The DNS results were obtained on the computational domain defined above at an extremely fine spatial grid resolution of 1280×512 and a temporal resolution of 2048 steps per (fundamental) disturbance period. To arrive at this resolution, computations were made on successively finer grids beginning from a coarse grid of 256×128. For each spatial resolution, an estimate of the temporal resolution necessary for stability was made based on stability analyses of model advection and diffusion equations. All computations except for that on the finest grid eventually "blew up" due to numerical instabilities associated with unresolved scales. In contrast, Fig. 7 shows instantaneous contours of constant density at $t_P = 18$ for the fully resolved computation. On the finest grid, the DNS computation required in excess of 20 CPU hours on a Cray C90. Consequently, calculations at a higher Reynolds number would have been impractical given the computational resources available.

The present fine-grid DNS represents one of the most accurate and highly refined computations of an unbounded shear layer of which we are aware, another being that of Colonius et al. (1995), and Fig. 7 affords considerable detail. It is interesting to note a striking correlation between the contours of constant density and those of constant vorticity (not shown due to space limitations). Both quantities clearly show the roll-up of the shear layer at the jet's edge into a vortex street and the subsequent pairing of adjacent vortices, phenomena common to unbounded shear flows. A similar comparison of vorticity and pressure contours is also most revealing. Not unexpectedly, the centers of low pressure correspond precisely with the centers of the large vortices. As adjacent vortices merge, the individual pressure lows are replaced by larger and stronger low pressure regions. High pressure regions lie between adjacent vortices.

LES: For LES of jet flow, the trick is to find an appropriate amount of eddy viscosity. If the LES subgrid-scale model is insufficiently dissipative, the computation will blow up. On the other hand, if the model is excessively dissipative, the instabilities that result in vortex shedding and pairing are suppressed or diminished. It appears possible, however, that an intermediate amount of dissipation will preserve the large-scale features of the flow while preventing numerical instabilities associated with unresolved scales. In particular, Figs. 7 and 7 present instantaneous contours of constant density and pressure, respectively, obtained from an LES computation with a spatial grid resolution of 432×192, coarser by a factor of approximately three in each direction than the DNS computation presented previously. The time is $t_P = 18$, and the temporal resolution is 1024 time steps per period. Because fully explicit time-advancement schemes typically yield over-resolution in time, practicality demands a filter width Δ that is approximately, say, an order of magnitude larger than the time step. Here, we used $\Delta/\Delta t = 8$ ($R_c = 0.125$). At this cutoff frequency, the maximum eddy viscosity was approximately eight times the maximum physical viscosity. Whereas the DNS calculation required 20 CPU hours, the 432×192 LES calculation required two CPU hours. (Calculations on the coarsest grid of 256×128, for which the computation eventually blew up, required only a matter of minutes.) Relative to the DNS results of Fig. 7, the shear-layer roll-up and pairing events of the moderately dissipative LES computation are retarded, but not prevented. Consequently, we believe the moderately resolved LES could serve as a computational platform for the investigation of jet noise. To this end and following Colonius et al. [3], we extract the compressible dilatation from the numerical solution: The instantaneous dilatation field at $t_P = 18$ of the moderately resolved LES computation is shown in Fig. 7. It would appear that, in terms of the dilatation, each large vortex appears as an acoustic quadrupole. These results suggest that significant acoustic radiation is associated with the large-scale vortices, in contrast to the view expressed by Tam (1995) for subsonic jets.

For the present work in progress, our primary objective has been to demonstrate the feasibility and practicality of time-filtered spatial LES. As one possible measure of success, we examine the resolved subgrid-scale stresses computed by the time-filtered subgrid-scale model, the principal component of which is presented in Fig. 7. For an LES computation, the magnitude of the resolved stresses can be viewed as a measure of ill resolution, or equivalently, as identifying the regions where additional dissipation is needed to prevent numerical instability. For the present time-filtered approach, these terms are well defined, judging by the apparent smoothness of the contours in the figure. In summary, these results suggest that a time-filtered dynamic subgrid-scale model could be developed. We suspect that dynamic modeling (Germano et al., 1991) would improve the present results by limiting the eddy viscosity only to regions where it is needed. For this reason, the dynamic approach is judged to be more appropriate for transitional flows, as was demonstrated for compressible flow, for example, in the work of El-Hady et al. (1993).

In closing, we comment that computations of 2D or axisymmetric unbounded shear flows are both less and more difficult than computations of 3D flows. Although the total computational requirements are lower for simulations in 2D, the resolution needed for those two dimensions may well be greater than for the same two dimensions of a 3D simulation. The reason is that, in 3D, the third dimension provides a path for relief of Reynolds stresses that cannot be relieved in 2D. Complete validation of the present time-filtered LES concept

and its application to aeroacoustics ultimately will require the consideration of fully 3D flows.

7 CONCLUSIONS

- Time-domain filtering for the residual-stress models of LES is a viable concept that should be investigated further. Preliminary results suggest that time-domain filtering may have significant advantages relative to conventional space-filtered approaches.
- The current baseline LES algorithm is one of a very few LES algorithms to exploit high-order numerical methods.
- The present subgrid-scale model, which involves time-domain filtering, might be improved for application to transitional flows by recasting it in a dynamic-model context (Germano et al., 1991).
- The present approach to LES appears to be applicable to aeroacoustics, as had been hoped.
- A thorough validation of the time-filtered LES approach and its usefulness to aeroacoustics will require LES of fully 3D flows.

ACKNOWLEDGEMENTS

In addition to the financial support of NASA Langley Research Center acknowledged on page 1, the computational support of the National Aerodynamic Simulator (NAS) at NASA Ames Research Center is also gratefully acknowledged. The author is also indebted to Drs. Gordon Erlebacher, Ugo Piomelli, and Klaus Adams for helpful discussions and clarifying insights.

References

[1] A. A. Aldama. *Filtering Techniques for Turbulent Flow Simulation.* Springer-Verlag, Berlin, 1990.

[2] D. A. Anderson, J. C. Tannehill, and R. H. Pletcher. *Computational Fluid Mechanics and Heat Transfer.* Hemisphere Publishing Company, 1984, pp. 391-394.

[3] T. Colonius, S. K. Lele, and P. Moin, "The Sound Generated by a Two-Dimensional Shear Layer: A Comparison of Direct Computations and Acoustic Analogies," CEAS/AIAA Paper No. 95-036.

[4] Y. M. Dakhoul and K. W. Bedford, "Improved Averaging Method for Turbulent Flow Simulation. Part I: Theoretical Development and Application to Burgers' Transport Equation," *Int. J. Num. Meth. Fluids*, Vol. 6, 1986, pp. 49-64.

[5] N.M. El-Hady, T.A. Zang, and U. Piomelli, "Dynamic Subgrid-Scale Modeling for High-Speed Transitional Boundary Layers," in *Engineering Applications of Large Eddy Simulations–1993*, eds. S.A. Ragab and U. Piomelli, FED-Vol. 1962, 1993, pp. 103-112.

[6] G. Erlebacher, M. Y. Hussaini, C. G. Speziale, and T. A. Zang, "Toward the Large-Eddy Simulation of Compressible Turbulent Flows," *J. Fluid Mech.*, Vol. 238, 1992, pp. 155-185.

[7] M. Germano, "Turbulence: The Filtering Approach," *J. Fluid Mech.*, Vol. 238, 1992, pp. 325-336.

[8] M. Germano, U. Piomelli, P. Moin, and W. H. Cabot, "A Dynamic Subgrid-Scale Eddy Viscosity Model," *Phys. Fluids A*, Vol. 3, 1991, pp. 1760-1765.

[9] S. K. Lele, "Compact Finite Difference Schemes with Spectral-Like Resolution," *J. Comput. Phys.*, Vol. 103, 1992, pp. 16-42.

[10] P. Moin and J. Jimenez, "Large-Eddy Simulation of Complex Turbulent Flows," AIAA Paper No. 93-3099, 1993.

[11] R. R. Mankbadi, M. E. Hayder, and L. A. Povinelli, "Structure of Supersonic Jet Flow and Its Radiated Sound," *AIAA J.*, Vol. 32, No. 5, 1994, pp. 897-906.

[12] W. H. Press, B. P. Flannery, S. A. Teukolsky, and W. T. Vetterling, *Numerical Recipes: The Art of Scientific Computing.* Cambridge University Press, Cambridge, 1986, pp. 436-444.

[13] C. D. Pruett, "A Semi-Implicit Method for Internal Boundary-Layer Flows," *Comp. Meth. Applied Mech. Eng.*, 1996, (to appear).

[14] C. D. Pruett, "Toward the Simplification of Dynamic Subgrid-Scale Models," paper submitted for the First AFOSR International Conference on Direct Numerical Simulation and Large-Eddy Simulation, to be held at Louisiana Tech Univ., Ruson, LA, Aug. 4-8, 1997.

[15] C. D. Pruett, T. A. Zang, C.-L. Chang, and M. H. Carpenter, "Spatial Direct Numerical Simulation of High-Speed Boundary-Layer Flows–Part I: Algorithmic Considerations and Validation," *Theoret. Comput. Fluid Dynamics*, Vol. 7, No. 5, 1995, pp. 49-76.

[16] J. J. Riley and R. W. Metcalfe, "Direct Numerical Simulation of a Perturbed, Turbulent Mixing Layer," AIAA Paper No. 80-0274, 1980.

[17] J.M. Seiner, "Advances in High-Speed Jet Aeroacoustics," AIAA Paper No. 84-2275, 1984.

[18] C. G. Speziale, G. Erlebacher, T. A. Zang, and M. Y. Hussaini, "The Subgrid-Scale Modeling of Compressible Turbulence," *Phys. Fluids A*, Vol. 31, No. 4, 1988, pp. 940-942.

[19] C. L. Streett and M. G. Macaraeg, "Spectral Multi-Domain for Large-Scale Fluid Dynamic Simulations," *App. Numer. Math.* Vol. 6, 1989/1990 pp. 123-139.

[20] R. D. Strum and D. E. Kirk, *First Principles of Discrete Systems and Digital Signal Processing.* Addison-Wesley, New York, 1988.

[21] C. R. Tam, "Supersonic Jet Noise," *Annu. Rev. Fluid Mech.*, Vol. 27, 1995, pp. 17-43.

[22] K. W. Thompson, "Time Dependent Boundary Conditions for Hyperbolic Systems," *J. Comput. Phys.*, Vol. 68, 1987, pp. 1-24.

FIGURES

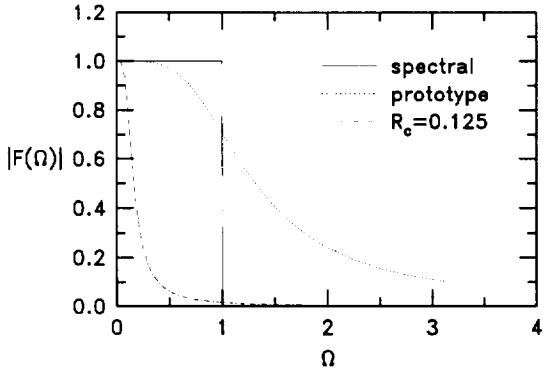

Figure 1. Transfer function of prototype second-order causal filter compared with spectral-cutoff transfer function.

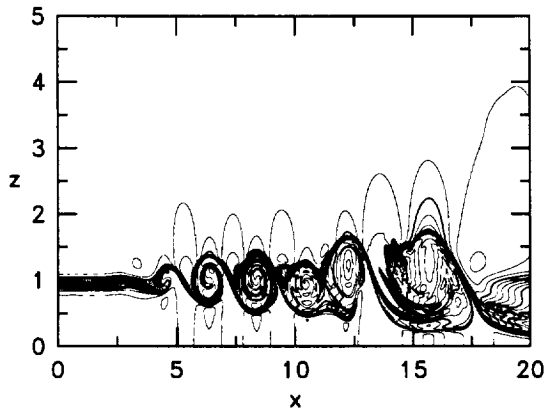

Figure 2. Contours of constant density obtained from well-resolved (1280 × 512) DNS calculation at $t_P = 18$. Flow is left to right. Jet centerline is along lower boundary of figure. Contour levels denote variations of $0.82 \leq \rho \leq 2.15$. Buffer domain shown.

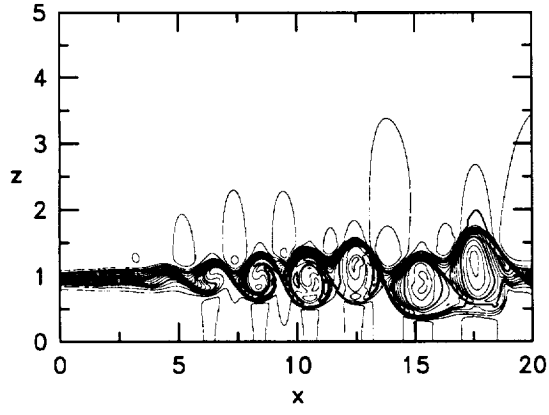

Figure 3. Contours of constant density obtained at $t_P = 18$ from LES of 432×192 grid resolution. Maximum eddy viscosity is 8 times that of physical viscosity. Relative to DNS. vortex roll-up and pairing events are retarded but not prevented. Contour levels denote variations of $0.95 \leq \rho \leq 2.13$. Buffer domain shown.

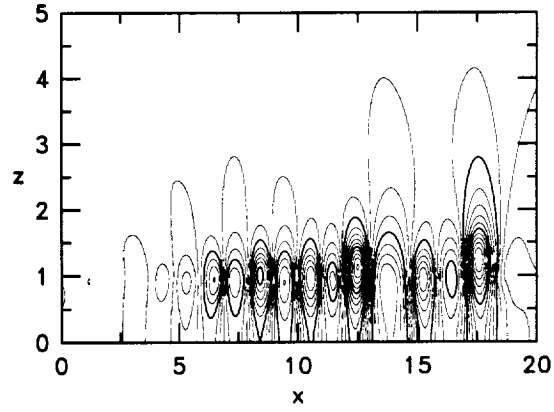

Figure 4. Contours of constant pressure obtained from LES calculation of resolution 432×192 at $t_P = 18$. Contour levels denote variations of $0.87 \leq p \leq 1.26$. Buffer domain shown.

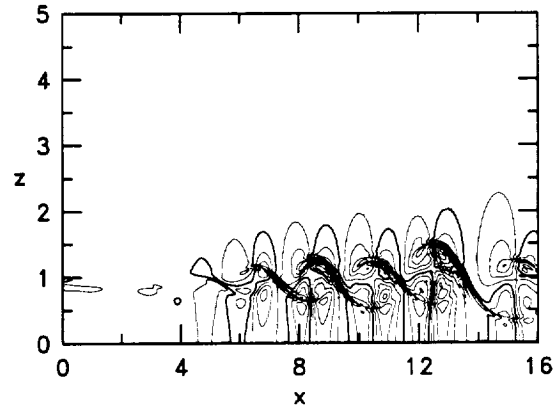

Figure 5. Isolevels of dilatation D obtained at $t_P = 18$ from LES of 432×192 grid resolution. Contour levels denote variations of $-0.10 \leq D \leq 0.13$. Buffer domain *not* shown.

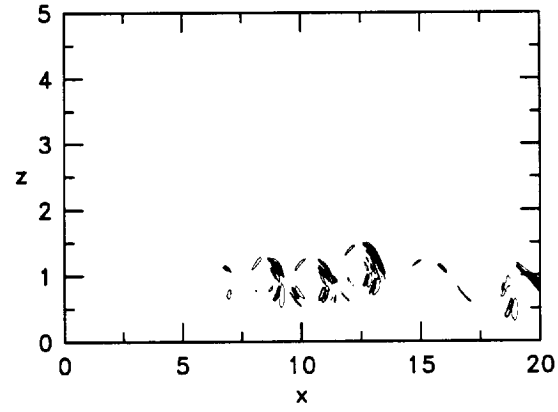

Figure 6. Principal component of resolved stresses obtained at $t_P = 18$ from LES of 432×192 grid resolution. Contour levels denote variations from -4.2×10^{-5} to 3.3×10^{-5}. Buffer domain shown.

TOWARD SIMPLIFICATION OF DYNAMIC SUBGRID-SCALE MODELS

C. David Pruett*
Department of Mathematics
James Madison University
Harrisonburg, VA, USA 22807

Abstract

We examine the relationship between the filter and the subgrid-scale (SGS) model for large-eddy simulations, in general, and for those with dynamic SGS models, in particular. From a review of the literature, it would appear that many practitioners of LES consider the link between the filter and the model more or less as a formality of little practical effect. In contrast, we will show that the filter and the model are intimately linked, that the Smagorinsky SGS model is appropriate only for filters of first- or second-order, and that the Smagorinsky model is inconsistent with spectral filters. Moreover, the Germano identity is shown to be both problematic and unnecessary for the development of dynamic SGS models. Its use obscures the following fundamental realization: *For a suitably chosen filter, the computible resolved turbulent stresses, properly scaled, closely approximate the SGS stresses.*

1 Introduction

By definition, direct numerical simulation (DNS) is the numerical solution of the Navier-Stokes equations without recourse to empirical models. In concept, the fluid motions are resolved down to the Kolmogorov length scale, at which eddies succumb to viscous dissipation. In general, the computational workload for fully-resolved DNS scales as Re^3, where Re is the Reynolds number. Consequently, for the complex, high-Reynolds-number flows of engineering interest, the computational requirements DNS are staggering and prohibitive.

In contrast, in large-eddy simulation (LES), the larger scales of motion are resolved in space and time on a moderately coarse grid; however, the effect of the subgrid-scale (SGS) motions on the evolution of the larger scales is modeled. In practice, the decomposition into resolved and unresolved scales is accomplished by a spatial (temporal) filtering operation with an associated cutoff length (time) scale Δ.

First introduced in the 1960's, LES has experienced a resurgence of interest since 1991, when dynamic SGS modeling was proposed by Germano and coworkers[6]. The advantages and difficulties associated with dynamic SGS models are now well established, and space does not permit elaboration. However, it is fair to say that the promise of dynamic modeling has not been fully realized largely because many of the proposed fixes to the shortcomings of dynamic models involve considerable additional complexity and computational overhead.

Here, our purpose is to examine the connection between the choice of the filter and the subgrid-scale (SGS) model, with an eye toward the simplification of dynamic SGS models.

From a review of the literature, it would appear that many practitioners of LES consider the link between the filter and the model more or less as a formality of little practical effect. Surprisingly little is written on this topic, Piomelli et al.[9] and Aldama[1] excepted. Specifically, regarding the conventional practice of LES, Piomelli et al.[9] observed: "In the past, however, the choices of model and filter have been regarded as completely independent." Recognizing that the behavior of the SGS model strongly depends on the choice of

*Research conducted under NASA Grant NAG-1-1802, monitored by Dr. Kristine R. Meadows, NASA Langley Research Center, Hampton, VA 23681-0001

the filter, they attempted to address the issue of filter-model consistency on the basis of physical arguments and *a priori* tests, which involve comparisons of the exact and modeled SGS stresses computed by fully resolved DNS. Here, we approach filter-model consistency from a mathematical point of view. From the present analysis come a number of revelations, some of which run counter to conventional wisdom.

In the next section, we discuss aspects of linear filters in general, focusing on their order properties. In the third section, starting from the Germano identity and in the context of a dynamic SGS model, we derive a simple but accurate approximation for the residual stresses. In the fourth section, we derive a similar result without first appealing to the Germano identity. In the fifth section, we briefly discuss the implications of these results. Conclusions are summarized in the final section.

2 Linear Filter Operators

Like differential operators, filter operators may be either continuous or discrete. Here, for brevity, we consider only continuous filters (which are also referred to as "analog"); however, the conclusions drawn for continous filters generalize immediately to linear discrete filters. Moreover, also for brevity, we consider only time-domain filters. However, the implications should apply to spatial filters as well.

Let $f(t,\vec{x})$ be a continous function of time and space, and let Δ, the "window" width, denote a characteristic time scale associated with the temporal linear filter $F[f(t),\Delta]$. As a specific example, consider the continuous, causal filter given by the integral equation

$$F\left[f(t,\vec{x}),\Delta\right] = \frac{1}{\Delta}\int_{t-\Delta}^{t} f(\tau,\vec{x})d\tau \tag{1}$$

From first principles of the Calculus, it is readily shown that $\lim_{\Delta\to 0} F[f(t),\Delta] = f(t)$. On the other hand, for a finite window Δ, the time-domain filter above tends to remove oscillations of high frequency relative to Δ while preserving low-frequency oscillations, which defines a "low-pass" filter. For applications to LES, we consider only low-pass filters.

The effect of a filter is most apparent in Fourier space. To each filter is associated a transfer function $H(\Omega)$ that quantifies the amplitude and phase effects of the filter on oscillations of dimensionless frequency $\Omega = \omega\Delta$. For example, the transfer function associated with Eq. 1, shown in Fig. 1, is readily obtained by directly integrating $F(e^{i\omega t},\Delta)$ for arbitrary ω. Figure 1 reveals some undesirable traits of the filter: the amplitude decay is not monotonic, the amplitude envelope decays slowly (like $1/\Omega$), and, consequently, the cutoff is gradual.

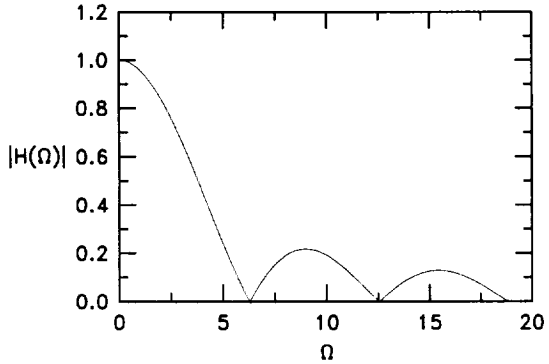

Figure 1. Transfer function of integral filter of Eq. 1.

Again by analogy to difference operators, to each filter operator is associated an order-property that quantifies the behavior of the filter as Ω tends toward zero. The order property is revealed by the leading non-zero term in Δ in the Taylor-series expansion of the filter. For example, for a function of time only, the Taylor-series expansion with respect to Δ of the filter of Eq. 1 is

$$F\left[f(t),\Delta\right] = f(t) - \frac{\Delta}{2}f'(t) + \frac{\Delta^2}{6}f''(t) + O(\Delta^3) \tag{2}$$

A class of causal time-domain filters more suitable for LES than Eq. 1 is that of the so-called Butterworth filters. Figure 2 compares the moduli of the transfer functions of prototypical Butterworth analog (BA) low-pass filters of orders 1, 2, and 4, each of which has a nominal cutoff frequency $\Omega_c' = 1$. The properties and design constraints of the first- and second-order low-pass BA prototypes can be found in Strum and Kirk[12]. The fourth-order BA prototype was developed by the author using Mathematica. The prototype BA filters shown in Fig. 2 are readily discretized and adapted to an arbitrary cutoff Ω_c.

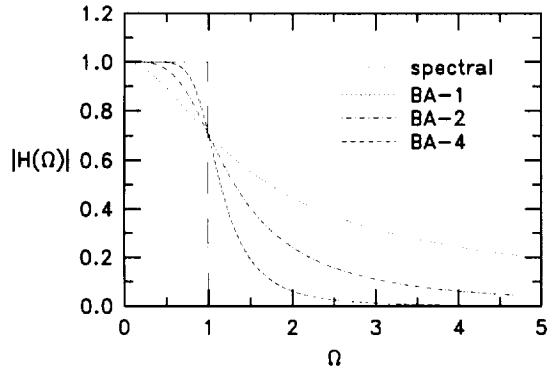

Figure 2. Comparison of Butterworth analog (BA) filters of orders 1, 2, and 4 with spectral (sharp cut-off) filter.

The order of a filter is closely related to the flatness of its transfer function at $\Omega = 0$. In general, for a filter of order n, $H^{(k)}(\Omega)|_{\Omega=0} = 0$ for all $0 < k \leq n$, but $H^{(n+1)}(0) \neq 0$. In particular, Butterworth filters manifest several desirable properties for applications to LES: 1) stability, i.e., $|H(\Omega)| \leq 1$; 2) their transfer functions decay monotonically with increasing Ω, and 3) their transfer functions are maximally flat near $\Omega = 0$. For comparison, Fig. 2 also presents the idealized transfer function of an analog spectral filter, which can be considered of infinite order.

For brevity in future discussions, let an overbar denote filtered quantities; that is, $\bar{f} \equiv F[f(t), \Delta]$ for some fixed Δ. From Figs. 1 and 2 it can be inferred that, except for the spectral filter, $\bar{\bar{f}} \neq \bar{f}$. It is also clear that the spectral ideal is more closely approximated as the order n increases. As a result, high-order temporal filters are problematic for practical applications to LES, because they necessitate the storage of relatively more time history. This may be a principal reason that, to date, time-domain filtering has been avoided by practitioners of LES, as hinted by Moin and Jimenez[8] in their survey paper.

One might naively assume (as did the author originally) that higher order is better. One of the more significant results of this work is to show that, in the context of LES, lower order filters are desirable for several reasons. This is particularly good news if one wants to consider the application of time-domain filters to LES, for example, as in Pruett[10].

To develop the results of the next sections, we make use of the Taylor series expansions of filter operators. For example, recall Eq. 1 above. More generally, assuming sufficient differentiability of u, any time-domain filter can be expanded as

$$\bar{u}(t, \vec{x}, \Delta) = u + c_1 \Delta u' + c_2 \Delta^2 u'' + c_3 \Delta^3 u''' + ... \tag{3}$$

where primes denote temporal partial derivatives. For spatially multi-dimensional filter operators, similar expansions could be derived; however, their Taylor expansions would, of course, be multi-dimensional. In general, a filter is of order n in Δ provided $c_n \neq 0$, but $c_k = 0$ for $1 \leq k < n$. Thus, Eq. 1, for example, defines a first-order filter. Similarly, one can show that both Gaussian and tophat physical-space filters are first order.

3 Conventional Dynamic SGS Modeling

In tensor notation, the linearly filtered Navier-Stokes equations are given by

$$\frac{\partial \bar{u}_i}{\partial x_i} = 0 \tag{4}$$

$$\frac{\partial \bar{u}_i}{\partial t} + \frac{\partial}{\partial x_j}(\bar{u}_i \bar{u}_j) = -\frac{1}{\rho}\frac{\partial \bar{p}}{\partial x_i} + \nu \nabla^2 \bar{u}_i + \frac{\partial \tau_{ij}}{\partial x_j} \tag{5}$$

where repeated indices imply summation, and τ_{ij} is the SGS (residual) stress tensor defined as

$$\tau_{ij} \equiv \overline{u}_i \overline{u}_j - \overline{u_i u_j} \tag{6}$$

Equation 6 is exact; inexactness enters only when the τ_{ij} are modeled. We focus now on dynamic modeling of the residual stresses.

Dynamic models[6] of the SGS stress tensor are rooted in the Germano[5] identity and typically exploit successive (spatial) "grid" and "test" filtering operations with associated length scales l and $\hat{l}$, respectively. To transition to temporal filtering, we explicitly assume that $\frac{\hat{\Delta}}{\Delta} = \frac{\hat{l}}{l} = r$, where $r > 0$ is a parameter. Typically, $r = 2$. The Germano identity relates the resolved turbulent stress tensor $\mathcal{L}_{ij}$ and the "subgrid" and "subtest" stress tensors, τ_{ij} and T_{ij}, respectively. Specifically,

$$\mathcal{L}_{ij} = T_{ij} - \hat{\tau}_{ij} \tag{7}$$

where

$$\mathcal{L}_{ij} \equiv \hat{\overline{u}}_i \hat{\overline{u}}_j - \widehat{\overline{u}_i \overline{u}_j} \tag{8}$$

and

$$T_{ij} \equiv \hat{\overline{u}}_i \hat{\overline{u}}_j - \widehat{\overline{u}_i \overline{u}_j} \tag{9}$$

The Germano identity is exact; moreover, its left-hand side is computible. It remains to model each of the terms on the right-hand side, which is frequently accomplished via the Smagorinsky eddy-viscosity model, namely

$$\tau_{ij} - \frac{1}{3}\delta_{ij}\tau_{kk} \approx 2Cl^2|\overline{S}|\overline{S}_{ij} \tag{10}$$

Here, δ_{ij} is the Kronecker delta, $\overline{S}_{ij}$ is the resolved-scale strain-rate tensor, $|\overline{S}| \equiv \sqrt{2\overline{S}_{ij}\overline{S}_{ij}}$, l is the characteristic length scale associated with the grid filter, and C is the model constant of primary interest. In general, a criticism of eddy-viscosity models is their implicit assumption that the principal axes of the residual stress and the resolved-scale strain-rate tensors are aligned (Moin and Jimenez[8]). Indeed, in a recent experiment that examined turbulent three-dimensional boundary-layer flow, Compton and Eaton[4] found considerable misalignment between residual-stress and strain-rate tensors in the near-wall region. They concluded that eddy-viscosity models are inappropriate for such flows. Moin and Jimenez[8] propose a more generally applicable model, for which each stress-tensor component has its own coefficient, namely

$$\tau_{ij} \approx (C_{ik}\overline{S}_{kj} + C_{jk}\overline{S}_{ki})l^2|\overline{S}| = \frac{1}{2}(C_{ik}\beta_{kj} + C_{jk}\beta_{ki}) \tag{11}$$

where

$$\beta_{ij} \equiv 2l^2|\overline{S}|\overline{S}_{ij} \tag{12}$$

We will refer to Eq. 11 as the "generalized residual-stress model." The generalized residual-stress tensor is symmetric; hence, six independent coefficients must be determined. In principle, these coefficients can be uniquely determined by the dynamic procedure of Germano et al.[6], as adapted to the generalized model by Moin and Jimenez[8]. We briefly describe the procedure below.

It is now assumed that the subtest stresses can also be modeled by Eq. 11 with the same coefficients C_{ij}, in which case

$$T_{ij} \approx (C_{ik}\hat{\overline{S}}_{kj} + C_{jk}\hat{\overline{S}}_{ki})\hat{l}^2|\hat{\overline{S}}| \tag{13}$$

(In the author's opinion, this assumption represents a considerable leap of faith, given that τ_{ij} and T_{ij} are not formal twins.) From Eqs. 7, 11, and 13, a set of integral equations for the coefficients C_{ij} follows, namely

$$2\mathcal{L}_{ij} \approx (C_{ik}\alpha_{kj} + C_{jk}\alpha_{ki} - C_{ik}\widehat{\beta}_{kj} - C_{jk}\widehat{\beta}_{ki}) \tag{14}$$

where

$$\alpha_{ij} \equiv 2\hat{l}^2|\hat{\overline{S}}|\hat{\overline{S}}_{ij} \tag{15}$$

We now exploit the Taylor-series expansion of the test filter to obtain a simple approximation to Eq. 14. For specificity, we use the filter of Eq. 1 and its expansion Eq. 2. Omitting details for brevity, we obtain the approximation

$$2\mathcal{L}_{ij} \approx (r^2-1)\left(C_{ik}\beta_{kj}+C_{jk}\beta_{ki}\right)+2L.O.E.+O(l^2\hat{\Delta}^2)=2(r^2-1)\tau_{ij}+2L.O.E.+O(l^2\hat{\Delta}^2) \tag{16}$$

where the leading-order error (L.O.E.) term in $\hat{\Delta}$ is given by

$$L.O.E.=-\frac{\hat{\Delta}}{4}\left[r^2\left(C_{ik}\frac{\partial\beta_{kj}}{\partial t}+C_{jk}\frac{\partial\beta_{ki}}{\partial t}\right)-\left(\frac{\partial C_{ik}\beta_{kj}}{\partial t}+\frac{\partial C_{jk}\beta_{ki}}{\partial t}\right)\right] \tag{17}$$

We conclude that

$$\tau_{ij}\approx\frac{\mathcal{L}_{ij}}{r^2-1}-\frac{L.O.E.}{r^2-1}+O(l^2\hat{\Delta}^2) \tag{18}$$

We now assume that the highest order term is insignificant. It remains to show that the second term (L.O.E.) on the right-hand side of Eq. 18 is of lesser significance (on average) than the first. We assume here that all quantities have been previously scaled by appropriate reference values, so that we are dealing only with dimensionless quantities. It particular, lengths have been scaled by the wavelength of the largest eddies, and time has been scaled by the large-eddy turnover time. From Eqs. 8 and 2, to leading order in $\hat{\Delta}$, the resolved turbulent stresses are given by

$$\mathcal{L}_{ij}=\frac{\hat{\Delta}^2}{12}\left(\frac{\partial\overline{u}_i}{\partial t}\right)\left(\frac{\partial\overline{u}_j}{\partial t}\right)+O(\hat{\Delta}^3) \tag{19}$$

In scaled variables, on the basis of reasonable assumptions and approximations (omitted for brevity), it can be argued that the L.O.E. above is relatively unimportant whenever the dimensionless frequency $\Omega\equiv\Delta\omega<<1$ (provided the filter is of first- or second-order, as will be shown). Specifically, for example, if $\Omega_c\approx 0.1$, an entirely reasonable value in practice, then, Eq. 18 is approximated simply as

$$\tau_{ij}\approx\frac{\mathcal{L}_{ij}}{r^2-1} \tag{20}$$

Remarkably, Liu et al.[7] arrive at a result similar to Eq. 20 from *experimental* measurements in a turbulent jet. Specifically, they obtain several components of the SGS stress tensor of a jet by two-dimensional particle velocimetry. Whereas eddy-viscosity closures correlate poorly with the measured residual stresses, the resolved stresses correlate well. They propose the simple stress-similarity model

$$\tau_{ij}=c_L\mathcal{L}_{ij} \tag{21}$$

where the coefficient c_L is empirically derived. For $r=2$, they obtain $c_L=0.45\pm0.15$ for a "clipped" (no backscatter) SGS model by matching the exact and modeled SGS dissipation rates. For a model without clipping the optimal coefficient is approximately unity (Meneveau, personal communication). Either way, their result corroborates our observation that the residual and resolved turbulent stresses should be highly correlated.

The implications of our present results for the practice of dynamic SGS modeling are both troubling and hopeful. Because the effects of numerator and denominator of the modeled residual stresses essentially "cancel" in the present analysis, dynamic SGS models, viewed in the present light, are ultimately *independent of the form of their underlying model* (whether Smagorinsky or otherwise)! This unanticipated result suggests that the whole concept of dynamic modeling needs re-examination.

In hindsight, it appears to the author that the basis of dynamic models in the Germano identity is fundamentally flawed. The Germano "identity" is actually tautological, having been derived simply by regrouping and renaming certain quantities from the starting point $\hat{\tau}_{ij}=\hat{\tau}_{ij}$. This is not to say that the idea of dynamic modeling is flawed, only that there is no necessity for the Germano identity, as will be shown. Moreover, not only is the Germano identity unnecessary, it results in the practical difficulty associated with the vanishing denominator of the model coefficient.

4 Alternate Approach to Dynamic Modeling

In light of the discussion above, it is natural to ask: *Can the residual stresses be modeled by the resolved turbulent stresses without appealing to the Germano identity?*

By applying the general Taylor expansion Eq. 3 to Eq. 6, we obtain

$$\tau_{ij} = (c_1^2 - 2c_2)u_i'u_j'\Delta^2 + (c_1c_2 - 3c_3)(u_i'u_j'' + u_j'u_i'')\Delta^3 + \text{H.O.T.} \tag{22}$$

where H.O.T. denotes higher order terms. Because the SGS-stress tensor τ_{ij} arises solely from the quadratic nonlinearity of the NS equations, it is quadratic at leading order in Δ, *provided that the filter is of either first- or second-order.* On the other hand, if the filter is of order $n > 2$, then τ_{ij} is of leading order n. Because the Smagorinsky model is of second-order in l (or equivalently, in Δ), it can be concluded immediately from Eqs. 10 and 22 that the model is appropriate only in the context of first- or second-order filters. Moreover, the use of Smagorinsky-based SGS models is totally inconsistent with spectral filters (which as we have said previously, can be considered of infinite order). This conclusion should hold regardless of whether filtering is accomplished in space or in the time domain. Our results are supported by experimental evidence. Liu et al.[7] find high correlations between τ_{ij} and $\mathcal{L}_{ij}$ when filtering is accomplished consistently with either Gaussian or physical-domain top-hat filters (both of which are first-order in our terminology). On the other hand, negligible correlations exist when a sharp cut-off filter is used in Fourier space (i.e., a spectral filter in our terminology).

Of fundamental importance in dynamic models is the resolved turbulent stress tensor $\mathcal{L}_{ij}$ (Eq. 8). As mentioned previously, the resolved turbulent stresses can be directly computed by filtering the resolved velocity fields $\bar{u}_i$. Let us now expand $\mathcal{L}_{ij}$ analogously to Eq. 22 above. To this end, we presume that the grid and test filters differ only in their respective filter widths. More precisely, if the grid filter is defined by Eq. 3, then the test filter is defined by

$$\hat{u}(t,\vec{x}) \equiv F\left[u(t,\vec{x}),\hat{\Delta}\right] = u + c_1(r\Delta)u' + c_2(r\Delta)^2u'' + c_3(r\Delta)^3u''' + ... \tag{23}$$

with the same coefficients c_i as in Eq. 3. From Eqs. 3, 8, and 23, and with the aid of Mathematica, it follows that

$$\mathcal{L}_{ij} = (c_1^2 - 2c_2)u_i'u_j'(r\Delta)^2 + (c_1^3r^2 - 2c_1c_2r^2 + c_1c_2r^3 - 3c_3r^3)(u_i'u_j'' + u_j'u_i'')\Delta^3 + \text{H.O.T.} \tag{24}$$

From comparisons of Eq. 22 and Eq. 24, we conclude that the SGS stresses can be approximated to leading order by the resolved stresses scaled by r^2; that is,

$$\tau_{ij} \approx \frac{\mathcal{L}_{ij}}{r^2} \tag{25}$$

How good is the approximation? Let the approximation error E be defined

$$E_{ij} \equiv \tau_{ij} - \frac{\mathcal{L}_{ij}}{r^2} \tag{26}$$

From Eqs. 22 and 24, we obtain

$$E_{ij} = \left[3c_3(r-1) + c_1c_2(3-r) - c_1^3\right]\Delta^3(u_i'u_j'' + u_j'u_i'') + \text{H.O.T.} \tag{27}$$

From Eqs. 22 and 27, we immediately conclude the following:

1. If the filter is of either first- or second-order in Δ, then the approximation error is of higher order (3) than is the SGS stress (2), and the approximation is likely to be reasonably accurate (given additional constraints to be addressed shortly).

2. On the other hand, for any filter of order $n > 2$, the approximation error is of the same order as τ itself; hence, τ is likely to vanish in the noise of the approximation.

3. If the filter is of order two ($c_1 = 0.0$, $c_2 \neq 0.0$) then

$$E_{ij} = 3c_3(r-1)\Delta^3(u_i'u_j'' + u_j'u_i'') + \text{H.O.T.} \tag{28}$$

4. Far from being inadmissible, as implied by the conventional dynamic modeling approach, $r = 1$ is *optimal* for second-order filters in that the leading error term vanishes.

5. Because the residual stresses can be approximated directly from the resolved turbulent stresses, the Germano identity is unnecessary for the development of dynamic SGS models.

5 Discussion

Although, for brevity, the present results were derived using time-domain filtering, similar results could have been obtained for spatial filtering, albeit by more arduous mathematics. For example, Eq. 19 is the time-filtered analog to the space-filtered result of Clark et al.[3] as interpreted by Speziale[11], who reports that

$$\mathcal{L}_{ij} = \frac{\hat{\Delta}^2}{12}\left(\frac{\partial \overline{u}_i}{\partial x_k}\right)\left(\frac{\partial \overline{u}_j}{\partial x_k}\right) + O(\hat{\Delta}^3) \tag{29}$$

Although Eqs. 20 and 25 are similar and in reasonable agreement for moderately large r, they are not identical. Whence the difference? Because the former originates from the Germano identity and the latter explicitly avoids it, we speculate that the discrepancy follows from the assumption that τ_{ij} and T_{ij} of Eq. 7 can both be modeled by formally identical models, despite some formal dissimilarity.

If both analysis and experiment conclude that the residual stresses correlate closely with the (computible) resolved stresses, then it is tempting to suggest for LES the use of SGS models that contain only scale-similarity terms. However, it is well known (e.g., Liu et al.[7]), that scale-similarity models alone are insufficiently dissipative, and such calculations are almost guaranteed to blow up, particularly if the numerical scheme is non-dissipative. Our interpretation of the situation is as follows: the SGS models of LES must unfortunately play two roles: one physical and one mathematical. Whereas scale-similarity models appear sufficient to capture the physics of SGS energy transfer, additional dissipation (e.g., a Smagorinsky-like term) is necessary for mathematical reasons; i.e., to stabilize the numerical scheme whenever resolution is marginal. These roles are somewhat separated by mixed models (e.g., Bardina[2]), which include both scale-similarity and dissipative terms.

Although our results are completely consistent with the experimental results of Liu et al.[7], they are only partially consistent with the DNS results of Piomelli et al.[9], whose *a priori* tests show good agreement between modeled and exact stresses both for a mixed model with a Gaussian filter and for the Smagorinsky model with a sharp cut-off filter. Whereas the former result is consistent with our findings, the latter is not. However, as Piomelli et al.[9] are careful to point out: "The fact that the SGS stress is essentially zero when the cutoff filter is used on the present [DNS] grid indicates that, with that filter, the grid may be capable of resolving the Reynolds stress and no model is needed." Thus, the inconsistency may be more apparent than actual. We are currently conducting *a priori* tests to further validate our present analysis.

6 Conclusions

1. Mathematically tautological, the Germano "identity" is suspect as a basis for dynamic SGS modeling.
2. A practical difficulty with dynamic SGS modeling, manifested in the vanishing denominator of the model coefficient, is directly attributable to the use of the Germano identity.
3. The Germano identity is not only problematic, it is an unnecessary basis for dynamic SGS models.
4. For first- or second-order filter operators, the computible resolved turbulent stresses, when properly scaled, closely approximate the residual stresses, without appeal to the Germano identity.

5. In general, filters of higher than second order are inconsistent with the Smagorinsky SGS model.
6. In particular, spectral filters are inconsistent with the Smagorinsky SGS model.
7. In LES, the SGS model plays two roles: one physical and one mathematical. To separate these roles, mixed models should be exploited. In mixed models, the scale-similarity term captures the physics and the dissipative term prevents numerical instability. Common experience with LES reveals that the scale-similarity term alone is insufficient.
8. The scaling of the scale-similarity term of mixed models should depend on the choice of the parameter r relating grid and test filter widths. This has been overlooked in practice.
9. A new model for the dissipative term, directly based on the computible resolved turbulent stresses, is sorely needed.

Acknowledgements

The author is grateful to Drs. Gordon Erlebacher of Florida State University; Kristine Meadows, Craig Streett, Michele Macaraeg, and Bart Singer of NASA Langley Research Center; and Bassam Younis of University College, London, for helpful discussions. He is also grateful to Dr. Sandip Ghosal of Los Alamos National Laboratory, to Dr. Klaus Adams of ZTH in Switzerland, and to Prof. Charles Meneveau of Johns Hopkins University for beneficial e-mail discussions and references regarding dynamic SGS modeling. Special thanks is due Prof. Ugo Piomelli of the University of Maryland for his time, insights, suggestions, clarifications, and numerous references. Any confusion that remains is entirely the author's.

References

[1] A. A. Aldama, *Filtering Techniques for Turbulent Flow Simulation*, Springer-Verlag, Berlin, 1990.

[2] J. Bardina, J. H. Ferziger, and W. C. Reynolds, "Improved Subgrid Scale Models for Large Eddy Simulation," AIAA Paper No. 80-1357, 1980.

[3] R. A. Clark, J. H. Ferziger, and W. C. Reynolds, "Evaluation of Subgrid-Scale Models Using an Accurately Simulated Turbulent Flow," *J. Fluid Mech.*, Vol. 91, 1979, pp. 1-16.

[4] D. A. Compton and J. A. Eaton, "Development of Near-Wall Statistics in a Three-Dimensional Turbulent Boundary Layers," in *Three-Dimensional Boundary Layers*, FED-Vol. 237, ASME, 1996.

[5] M. Germano, "Turbulence: The Filtering Approach," *J. Fluid Mech.*, Vol. 238, 1992, pp. 325-336.

[6] M. Germano, U. Piomelli, P. Moin, and W. H. Cabot, "A Dynamic Subgrid-Scale Eddy Viscosity Model," *Phys. Fluids A*, Vol. 3, 1991, pp. 1760-1765.

[7] S. Liu, C. Meneveau, and J. Katz, "On the Proporties of Similarity Subgrid-Scale Models as Deduced from Measurements in a Turbulent Jet," *J. Fluid Mech.*, Vol. 275, No. 83, 1994, pp. 83-119.

[8] P. Moin and J. Jimenez, "Large-Eddy Simulation of Complex Turbulent Flows," AIAA Paper No. 93-3099, 1993.

[9] U. Piomelli, P. Moin, and J. H. Ferziger, "Model Consistency in Large-Eddy Simulation of Turbulent Channel Flow," *Phys. Fluids A*, Vol. 31, No. 7, 1988, pp. 1884-1891.

[10] C. D. Pruett, "Time-Domain Filtering for Spatial Large-Eddy Simulation," to be presented at the 3rd Symposium on Transitional and Turbulent Compressible Flows, Annual Summer Meeting of the Fluids Engineering Division of the ASME, Vancouver, BC, June 22-26, 1997.

[11] C. G. Speziale, "Galilean Invariance of Subgrid-Scale Stress Models in the Large-Eddy Simulation of Turbulence," *J. Fluid Mech.*, Vol. 156, 1985, pp. 55-62.

[12] R. D. Strum and D. E. Kirk, *First Principles of Discrete Systems and Digital Signal Processing*, Addison-Wesley, New York, 1988.